Title

Effects of β-diketone antibiotics on F1-zebrafish (Danio rerio) based on high throughput miRNA sequencing under exposure to parents

Authors

Zheng, Yuansi
Lin, Jiebo
Li, Jieyi
et al.

Publication Date

2016-12-01

DOI

10.1016/j.chemosphere.2016.07.057

Peer reviewed

Chemosphere 164 (2016) 41–51

Contents lists available at ScienceDirect

Chemosphere

journal homepage: www.elsevier.com/locate/chemosphere

Effects of β-diketone antibiotics on F1-zebrafish (*Danio rerio*) based on high throughput miRNA sequencing under exposure to parents

Yuansi Zheng [a], Jiebo Lin [a], Jieyi Li [a], Haifeng Zhang [a], Weiming Ai [a], Xuedong Wang [b, **], Randy A. Dahlgren [b], Huili Wang [a, *]

[a] College of Life Sciences, Wenzhou Medical University, Wenzhou 325035, China
[b] Key Laboratory of Watershed Sciences and Health of Zhejiang Province, Wenzhou Medical University, Wenzhou 325035, China

HIGHLIGHTS

- Toxicity of DKAs to zebrafish was assessed by miRNA-seq and bioinformatics analyses.
- 193 mature miRNAs were differentially expressed in three comparison groups.
- A potential network was plotted between 11 positive miRNAs and their target genes.
- Expression of miR-124 and -499 in W-ISH was consistent with qRT-PCR and miRNA-seq.
- DKA exposure induced severe histopathological changes in F0-zebrafish ovary tissue.

ARTICLE INFO

Article history:
Received 14 May 2016
Received in revised form
16 July 2016
Accepted 18 July 2016
Available online 28 August 2016

Handling Editor: David Volz

Keywords:
miRNA
β-diketone antibiotics (DKAs)
Zebrafish
Small RNA
High throughput sequencing
Target genes

ABSTRACT

The toxicity of β-diketone antibiotics (DKAs), a class of "pseudo-persistent" environmental pollutants, to F0-zebrafish (*Danio rerio*) was investigated using 7-dpf F1-zebrafish miRNA sequencing and bioinformatics analyses. Based on relative expression, 47, 134 and 118 of 193 mature miRNAs were differentially expressed between control *vs* 6.25 mg/L, control *vs* 12.5 mg/L and 6.25 *vs* 12.5 mg/L treatments, respectively. Utilizing three databases, 2523 potential target genes were predicted, and they were assigned to 19 high-abundance KEGG pathways and 20 functional categories by COG analysis. Among 11 significantly differential expression and high-abundance miRNAs, the expression levels for 7 miRNAs (miR-144, -124, -499, -125b, -430b, -430c and -152) assessed by qRT-PCR were consistent with those determined by sRNA-seq. A potential network was plotted between 11 miRNAs and their target genes based on differential expression and binding effectiveness. The high degree of connectivity between miRNA-gene pairs suggests that these miRNAs play critical roles in zebrafish development. The expression of miR-124 and miR-499 in whole-mount *in situ* hybridization was in general agreement with those from qRT-PCR and miRNA-seq and were DKA concentration-dependent. DKA exposure induced severe histopathological changes and damage in F0-zebrafish ovary tissue, as reflected by an increased number of early developmental oocytes, irregular cell distribution, decreased yolk granules, cytoplasmic shrinkage, cell lysis in mature oocytes, and dissolution of internal corona radiata. Chronic DKA exposure affected reproduction of F0-zebrafish and development of F1-zebrafish. These observations demonstrate the toxic effect transfer relation across parent and their offspring, and enhance our understanding of drug-induced diseases.

1. Introduction

The β-diketone antibiotic compounds (DKAs), including fluoroquinolones (FQs) and tetracyclines (TCs), are prominent constituents in pharmaceuticals and personal care products. They are widely used in humans and veterinary practice to prevent and treat a large variety of infectious diseases (Alavi et al., 2015). The

* Corresponding author.
** Corresponding author.
E-mail address: whuili@163.com (H. Wang).

http://dx.doi.org/10.1016/j.chemosphere.2016.07.057
0045-6535/

widespread and frequent application of DKAs leads to "pseudo-persistent" in the environment, even though the half-lives for most DKA species are relatively short (~8 h) (Yoon et al., 2010). As a result, DKAs maintain background concentrations in the environment at ng/L to mg/L levels. DKAs originate in the environment from sources such as hospital sewage where large temporal variations in concentrations are observed: 3.6–101.0 mg/L for ciprofloxacin, 0.2–7.6 mg/L for ofloxacin, and 0.6–6.7 mg/L for doxycycline (Lindberg et al., 2004). What is noteworthy is the relatively high concentration (up to 0.355 mg/L) of ofloxacin found in hospital and residential effluent in New Mexicol (Brown et al., 2006). Golet et al. (2001) determined concentrations of ciprofloxacin and norfloxacin in real-world environmental waters in the concentration range of 249–405 ng/L and 45–120 ng/L, respectively. Consequently, DKAs pose a potential threat to aquatic organisms and human health due to their prevalence and mixed exposure in the environment.

Long-term exposure to low-doses of DKA mixtures can induce behavioral, biomarker and histopathological changes resulting in the origin of human diseases (Wang et al., 2016a,b). Therefore, the toxicological effects of DKAs have raised great concern in the fields of environmental, ecological and health sciences (Hagenbuch and Pinckney, 2012). With respect to detoxification metabolism, studies found that DKAs affected the activities of cytochrome P450, acetylcholinesterase (AChE) and superoxide dismutase (SOD) (Wang et al., 2014). Some DKAs, such as TCs, were found to be more toxic to aquatic organisms than FQs based on their inherent chemical properties (Ambili et al., 2012). Previous investigations by our group demonstrated that DKAs induced deleterious effects on the zebrafish nervous system and led to abnormal behavior and neurotoxicity (Wang et al., 2016a,b), as well as changes in heart development and skeletal muscle formation (Zhang et al., 2016). Wang et al. (2014) concluded that DKA exposure to F0-zebrafish embryos resulted in a series of developmental toxicity to F1-zebrafish, such as pericardial edema, uninflated swim bladder and yolk sac edema. FQ exposure was also reported to reduce the fertility and cloacal gland area in male Japanese quail (Mohan et al., 2004). Administration of tetracycline caused a reduction in the epididymal sperm motility, percentage of live spermatozoa, sperm count, and an increase in abnormal sperm morphology, as well as induction of adverse histopathological changes in the testes of African catfish (*Clarias gariepinus*) (Farombi et al., 2008). Tetracycline treatment of preovipositional *Otiorhynchus sulcatus* females specifically inhibited egg hatching and influenced reproduction of *Wolbachia*-infected parthenogenetic *O. sulcatus* females. However in *vivo* experiments, changes in metabolic transformation and distribution of DKAs make reproductive toxicity research more complicated (Melvin et al., 2014). Therefore, it is challenging to explore chronic toxicological effects of DKA exposure in studies evaluating reproductive risk.

In recent years, omics technology provides a novel approach for assessing pollutant toxicology in model organisms. MicroRNAs (miRNAs) are small non-coding RNAs that post-transcriptionally regulate gene expression by inducing cleavage of their target mRNA or by inhibiting their translation (Krol et al., 2010). Bhattacharya et al. (2016) found that miRNAs act as regulators in most biological processes, and as modulatory factors in developmental processes of zebrafish. Rapamycin exposure to zebrafish embryo resulted in significant suppression of melanocyte development and senescence-associated beta-galactosidase (SA-β-gal) activity, and perturbed the development of intersegmental vessels (ISVs) due to expression changes in zTOR-associated miRNAs (Khor et al., 2016). However, few studies have examined the reproductive toxicological effects from mixed DKA exposure, especially using next generation miRNA-sequencing techniques. Therefore, in this study we screened the significantly differential expression and high-abundance miRNAs based on miRNA-sequencing analyses, which are hidden in the genomic information and regulate target genes at the transcriptional level due to DKA exposure to zebrafish.

Zebrafish (*Danio rerio*) are a preferred model organism in human health risk and environmental toxicology research due to their tiny size, transparent embryo and rapid external embryonic development and high genetic and physiologic homology with humans (Sipes et al., 2011). Therefore, we chose zebrafish as a model organism to investigate the effects of DKA exposure on reproduction of F0-zebrafish and development of F1-zebrafish. This study aimed to screen and identify the significantly differential expression and high-abundance miRNAs from 7-dpf F1-zebrafish by miRNA sequencing after chronic DKA exposure to F0-zebrafish. Next, we systematically analyzed the functions of the screened miRNAs and their regulatory target genes. The functions of genes targeted by 193 mature miRNAs, which were differentially expressed (p-value ≤ 0.05, $\log_2$(fold-change) ≥ 1 or ≤ -1) between control and treatment groups, were elucidated by GO annotation, KEGG pathway analysis and COG protein classification. The expression was verified using qRT-PCR for 11 significantly differential expression and high-abundance miRNAs ($100 \leq$ FPKM ≤ 110000), and their potential target genes and regulatory network were predicted using DIANA miRPath software (v.2.0) (Vlachos et al., 2012). Seven miRNAs were consistent between qRT-PCR and sRNA-seq. Finally, *in situ* hybridization (ISH) was conducted to characterize the spatial expression pattern of miRNAs in F0-zebrafish ovary and whole-mount *in situ* hybridizations (W-ISH) in 7-dpf F1-zebrafish. Histopathological observation on F0-zebrafish ovary was performed to investigate structural changes due to DKA exposure. This study systemically evaluates the reproductive toxicity to zebrafish under the joint exposure of FQ and TC mixtures, and also enhances our understanding of drug-induced diseases.

2. Materials and methods

2.1. Ethics statement

All experimental protocols involving zebrafish followed the guidelines of the Institutional Animal Care and Use Committee (IACUC) at Wenzhou Medical University, Wenzhou, China. All zebrafish surgery was performed on ice to minimize suffering.

2.2. Chemical reagents

Certified DKA reference standards were sourced from Amresco (Solon, OH, USA) and used as received: ofluoxacin (CAS No. 82419-36-1, purity of 99%), ciprofloxacin (85721-33-1, 99%), enrofloxacin (93106-60-6, 99%), doxycycline (24390-14-5, 99%), chlortetracycline (64-72-2, 95%) and oxytetracycline (79-57-2, 99%). The chemical structures and molecular weights of the DKAs are shown in Fig. S1.

2.3. Zebrafish maintenance, embryonic collection and exposure experiment

Adult wild type zebrafish (AB strain) were purchased from a local supplier and adapted to the laboratory with a light/dark, 14 h/10 h cycle in a circulation system with dechlorinated tap water (pH 7.0–7.5) at a constant temperature (28 ± 0.5 °C). Zebrafish were fed twice daily with live *Artemia* (Jiahong Feed Co., Tianjin, China) and dry flake diet (Zeigler, Aquatic Habitats, Apopka FL, USA). Before spawning, male and female zebrafish (1:1) were paired in spawning boxes overnight. Once the light was turned on the following

morning, spawning was induced. Embryos were collected at 0.5 h post fertilization (hpf), and the fertilized and normal embryos were washed three times with embryo medium (EM) and incubated in EM, the composition of which was reported by Huang et al. (2004). Embryos at 6 hpf were exposed to control and two DKA treatments (6.25 and 12.5 mg/L) composed of the six DKA species listed above with equal weight concentrations and equal volumes of each DKA species. The DKA-exposure concentrations (6.25 and 12.5 mg/L) were selected according to dosage responses in our preliminary experiments. DKA working solutions were freshly prepared by dissolving the mixed standards containing the six DKA species in dechlorinated tap water. The 100% DKA-exposure solutions were renewed each day for the duration of the experimental period. The control (survival rates >95%) and DKA-exposure treatment groups were performed using 3 biological replicates ($n = 3$) and 3 technological replicates to assess accuracy and reproducibility. Each treatment included 3 tanks, which represented 3 biological replicates. In total, 9 tanks were used for the experimental treatments (control and two DKA-exposed treatments). Each tank including 40 zebrafish was equipped with an air pump and periodically cleared of fecal residue and any dead fish. The dechlorinated tap water (4 L) was added to a standard tank (27 cm length × 17.5 cm width × 21.5 cm height) for breeding zebrafish.

2.4. Health conditions adult zebrafish, RNA extraction, construction of small RNA library and sequencing

After 90 days of DKA exposure, the sexually mature zebrafish in control and DKA-exposed groups were randomly selected, and 50 zebrafish (25 male and 25 female) for each group were anesthetized on ice to minimize suffering. An electronic balance and vernier caliper (AUW320, Shimadzu, Japan) were used to measure zebrafish weight and length, respectively. Subsequently, body mass index (BMI) of males and females were calculated in each group. Twenty F1-zebrafish at 7-dpf for each group (control and two DKA-exposure treatments) were collected, homogenized in liquid nitrogen using a glass homogenizer and used for miRNA sequencing and qRT-PCR experiments. Additionally, 9 F1-zebrafish at 7-dpf for each group were used for ISH and W-ISH, and 9 F0-zebrafish at 90-dpf for each group were applied for pathological observations. Total RNA was extracted using a RNeasy Plant Mini Kit (Qiagen, Germany) and treated with DNase I using RNase Free Dnase Set (Qiagen, Germany) according to manufacturer's instructions. RNA purity was measured by the Nanodrop method with minimum requirements set to $OD_{260}/OD_{280} > 1.8$ and $OD_{260}/OD_{230} > 1.5$. The RNA integrity number (RIN >8) was used to develop the small RNA sequencing libraries. The sRNA libraries were constructed using the following steps: (1) Total RNA was purified by polyacrylamide gel electrophoresis (PAGE) to ensure that the RNA molecules were of the desired size range; (2) RNAs were ligated to the 3p and 5p adapters, and then transcribed to cDNA for PCR amplification to generate a cDNA library for Illumina sequencing; and (3) These libraries were used for paired-end sequencing using an Illumina Hiseq2000/2500 according to manufacturer's instructions (LC Sciences, USA). Small RNA library sequencing was completed by Hangzhou LC-Bio Co. (Hangzhou, China).

2.5. Bioinformatics analyses

2.5.1. Screening of differential miRNAs and prediction of target genes

Raw reads were initially processed into clean full-length reads by clipping adapters, trimming low-quality reads, and removing reads either shorter than 17 nt or longer than 25 nt. The valid reads were mapped to the miRbase database using Illumina's Genome Pipeline software (San Diego, CA, USA) and ACGT101-miR V4.2 software (LC Sciences, Houston, TX, USA). The relative abundance of transcripts was measured by the normalized small RNA-seq fragment counts. The measurement of Fragment Per Kilobase of exon per Million fragments mapped (FPKM) was applied for determining expression patterns of miRNAs among different treatments. The fold-change between different treatment groups was calculated on the basis of the equation: fold-change $= \log_2$(treat/control); a measure commonly used to quantify changes in the expression level of a gene (Zhao et al., 2015).

Three miRNA target prediction databases were used to assess the targets of differentially expressed miRNAs: TargetScan (http://www.targetscan.org/), MicroCosm (http://www.ebi.ac.uk/enright-srv/microcosm/htdocs/targets/v5/), and miRanda (http://www.microrna.org/). Only the targets commonly predicted by all three databases were considered reliable. For the sake of functional annotation of the genes targeted by the miRNAs, Gene Ontology (GO) (http://www.geneontology.org/) and Kyoto Encyclopedia of Genes and Genomes (KEGG) functional classification (http://www.genome.jp/kegg/) were performed using the web-based tool, Database for Annotation, Visualization and Integrated Discovery (DAVID, http://david.abcc.ncifcrf.gov/)(Huang et al., 2009). To obtain more information on the functions of differentially expressed genes, COG (Cluster of Orthologous Groups of proteins) classification was assessed to provide an intuitive understanding of the related functions for the significant differentially expressed genes using online software (http://www.ncbi.nlm.nih.gov/COG).

2.5.2. Analysis of significantly differential expression and high-abundance miRNA expression using qRT-PCR

qRT-PCR of mature miRNAs was performed to validate the sequencing results. We used the All-in-OneTM miRNA qRT detection system (Genecopoeia) followed by SYBR Green PCR (Bio-Rad) analysis to confirm and measure the expression of the screened significant differentially expressed miRNAs. The F0-zebrafish (6 hpf) were exposed to DKAs for 90 d, but F1-zebrafish (7 dpf) were not exposed to DKAs. The forward primers for the screened miRNAs were designed and synthesized by Sangon Biotech (Shanghai, China) and the reverse primers were the universal reverse primers provided by Genecopoeia with U6 as the endogenous reference (Table S1). All PCR reactions were performed for three biological replicates and each biological replicate included three technical replicates. Bio-Rad CFX Manager software was used to analyze the results from qRT-PCR. The relative changes in miRNAs expression were analyzed using the $2^{-\Delta\Delta CT}$ relative quantification method (Fu et al., 2006).

2.5.3. Potential target gene prediction of significantly differential expression and high-abundance miRNAs, and cluster and pathway analyses

DIANA miRPath (v.2.0) was performed to predict the potential target genes and pathways of miRNAs with significant differential expression. As zebrafish genes were not included in the current version of DIANA miRPath, prediction was conducted using human miRNAs. The *p*-value threshold was 0.05 and MicroT threshold was 0.860 (http://www.microrna.gr/miRPathv2). Cluster analyses of differentially expressed miRNAs were used to determine the clustering model of miRNA regulation under different experimental conditions. Based on the degree of similarity for miRNA expression profiles, cluster analyses can visually demonstrate representation of gene expression in different samples, thereby obtaining biologically relevant information (MEV4-9 software, http://www.tm4.org/mev.html). Cytoscape (v3.0.1) was applied for creating the potentially important networks for genes and miRNAs.

2.6. Whole-mount in situ hybridizations (W-ISH)

W-ISH was performed to characterize the spatial expression of miRNAs in 7-dpf F1-zebrfish after DKA exposure of F0-zebrafish for 90 days; the F1-zebrafish were not further exposed to DKAs. The 7-dpf F1-zebrafish were used for W-ISH including 3 biological replicates (9 zebrafish for each biological replicate), and each biological replicate was comprised of 3 technological replicates. The digoxigenin (DIG)-labeled antisense cDNA probe was synthesized by Sangon Biotech (Shanghai, China). W-ISH was performed using the method detailed by Thisse and Thisse (2008). Briefly, larvae at 7-dpf were fixed in 4% paraformaldehyde (Sigma-Aldrich, Saint Louis, MO, USA) at 4 °C overnight, then dehydrated with graded alcohol and preserved. The larvae were rehydrated prior to further testing. In order to increase the permeability of embryos, the embryos were treated with proteinase K. Subsequently, embryos were pre-hybridized and incubated for 2–5 h at 65 °C, then hybridized overnight at 65 °C with a probe concentration of 4 μg/mL. After rinsing the samples the next day, samples were incubated with an *anti*-digoxigenin antibody (Roche Diagnostics, Indianapolis, IN, USA) at a 1:5000 dilution. Nitroblue tetrazolium/5-bromo-4-chloro-3-indolyl phosphate (NBT/BCIP, Roche) was used as the enzymatic substrate.

2.7. In situ hybridizations (ISH)

To further explore the spatial expression of miRNAs in the ovary of F0-zebrafish, ISH was performed in 3 biological replicates (9 zebrafish for each biological replicate) and each biological replicate was comprised of 3 technological replicates according to Yao et al. (2010). Briefly, ovarian cryosections were prehybridized for 6 h at 65 °C with 700 μL prehybridization buffer (50% formamide, 5× saline sodium citrate, 5× Denhardt's, 200 μg/mL yeast RNA, 500 μg/mL salmon sperm DNA, 2% Roche blocking reagents, and diethylpyrocarbonate-treated water). The ovarian sections were then overlaid with 150 μL hybridization buffer (prehybridization buffer containing 1 pmol probes) and incubated overnight at 65 °C in a humidified chamber. After hybridization, the sections were washed 3 times with B1 buffer. The *anti*-digoxigenin-alkaline phosphatase fragments of antigen-binding fragments (Roche, Indianapolis, IN; 1:2500) and nitroblue tetrazolium and 5-bromo-4-chloro-3-indolyl phosphate (Promega) were used to detect the hybridization signals, which were quantified by Image-Pro Plus 6.0 Software (Media Cybemetics).

2.8. Histopathological observation of zebrafish ovary

After 90 days of DKA exposure (0, 6.25 and 12.5 mg/L), F0-zebrafish were used for paraffin-section histopathological observations. Zebrafish were dissected according to the guidelines of IACUC at Wenzhou Medical University. The ovary was dissected and fixed in 4% paraformaldehyde (PFA) overnight. Subsequently, tissues were paraffin-embedded followed by section-drying and haematoxylin and eosin (H&E) staining using standard protocols. Tissue structure damage was observed by optical microscope (DM2700M, Leica, Germany). To observe structural changes in detail, the dissected ovary was further cut into 1 mm^3 tissue blocks and fixed in glutaraldehyde at 4 °C. A series of pretreatment procedures, such as poaching, fixing, dehydrating, embedding and sectioning, were carried out according to Sendzik et al. (2010). The treated ovary samples were observed using transmission electron microscopy (TEM10, Zeiss, Jena, Germany).

2.9. Statistical analysis

The experimental data were reported as the mean ± SD (standard deviation). Each experimental group (0, 6.25 and 12.5 mg/L DKAs) contained three biological replicates, and each biological replicate was comprised of three technological replicates to assess accuracy and reproducibility. The number of zebrafish used in each biological replicate was 20 for qRT-PCR, 9 for W-ISH, 9 for ISH and 9 for histopathological observation, respectively. Post-hoc Tukey's tests were used for multiple comparisons among the different experimental groups. All statistical analyses were conducted with SPSS 18.0 (SPSS, Chicago, USA) using a $p < 0.05$ or $p < 0.01$ significance level, unless otherwise stated.

3. Results

3.1. Health conditions on adult zebrafish after chronic DKA exposure, miRNAs-Seq of F0-embryo and bioinformatics analyses

In the control group, zebrafish weight, length, proportion of female and male, and BMI were in the normal range, and in addition the mortality rate was less than 2% in the whole DKA-exposed process (6-hpf to 90 dpf). In contrast, DKA exposure led to increasing proportion of female and male, decreasing body mass at 6.25 ($p < 0.01$) and 12.5 mg/L ($p < 0.05$) treatments in female zebrafish. No significant differences were observed for BMI in male zebrafish, but the significant differences ($p < 0.01$) were found in female zebrafish between DKA-exposed treatments and control (Fig. S2). In total, 10,117,347, 9,818,830 and 12,049,949 raw reads were acquired, respectively, under the different DKA-exposure treatments (0, 6.25 mg/L and 12.5 mg/L) from the three miRNAs libraries by Illumina sequencing. Low quality reads were removed, which included 5′ contaminants, those missing the 3′ primer or insert tag, sequences with a poly A tail, and those shorter than 17 nt and longer than 25 nt. As a result, 8,141,146 (representing 312,735 unique sequences; control), 8,687,210 (representing 251,508 unique sequences; 6.25 mg/L), and 10,569,566 (representing 441,938 unique sequences; 12.5 mg/L) valid reads in the 17 to 25 nt size range were isolated for further analysis (Table S2). The sRNAs from the three libraries were similar, and the unique sRNA reads were mainly distributed in the 20–24 nt range, among which 22 and 23 nt accounted for 41.8% and 20.0% of total unique sRNA reads, respectively. The 22-nt sRNAs were the most abundant with the length distribution of counts of sequ-seqs and unique miRNAs displaying a normal distribution (Fig. S3C).

3.2. Screening for differentially expressed miRNAs

After removing sequencing adapters for unique sequences and repeating associate sRNA, and discarding rRNA, tRNA, snRNA and snoRNA, we further mapped the valid reads to the miRbase database (http://mirbase.org/index.shtml). A total of 193 mature miRNAs were differentially expressed (p-value $\leq$ 0.05, |fold change| $\geq$ 1) between control and treatment groups (Fig. S3A), and they were classified as either conserved miRNAs or non-annotated sRNAs. The conserved miRNAs represented the matched sequences in miRBase, which were further categorized into group 1 (42.5%), group 2 (4.2%), and group 3 (30.1%), and the non-annotated sRNAs were used to identify candidate novel miRNAs and classified as group 4 (23.3%). Group 1 contained the most components of the 193 miRNAs (Table S3). According to the relative expression levels of miRNAs, 47, 134 and 118 of the 193 miRNAs were differentially expressed between control *vs* 6.25 mg/L, control *vs* 12.5 mg/L and 6.25 *vs* 12.5 mg/L treatments, respectively (Fig. S3A). Consequently, there were repeat miRNAs in different comparison groups.

3.3. Target gene prediction and functional annotation

We obtained target genes from three databases (TargetScan, MicroCosm and miRanda) and only the targets commonly predicted by all three databases were considered reliable. Among the 193 matured miRNAs, 2523 potential target genes were successfully predicted (Fig. S3B). GO and KEGG functional classification were performed to annotate the potential functions for these target genes. The predicted target genes were clustered into cellular components, biological processes and molecular functions by GO analysis. The cellular components were mainly associated with cell and cell part, the biological processes were primarily involved in cellular and metabolic processes, and the molecular function analysis indicated major involvement in catalytic processes and binding (Fig. S4).

By KEGG pathway analysis, the target genes for the 193 miRNAs were mainly assigned to 19 high-abundance KEGG pathways, among which three main pathways, Focal adhesion (ko04510), MAPK signaling (ko04010) and Endocytosis (ko04144), were the majority of the genes (Fig. 1A). COG analysis (ftp://ftp.ncbi.nih.gov/pub/COG/) provided additional information on the ortholog of target genes and functional classification for the differentially expressed genes. We performed COG protein functional prediction and classified these genes into 20 functional categories (Fig. 1B). Signal transduction mechanisms represented the highest proportion of gene functions, followed by transcription, post-translational modification, protein turnover, chaperones, cell cycle control, cell division chromosome partitioning, intracellular trafficking, secretion and vesicular transport.

3.4. Validation of miRNA expression by qRT-PCR

Eleven significantly differential expression and high-abundance miRNAs were screened by qRT-PCR analyses with the signal of β-actin as a stable reference gene to validate the consistency between qRT-PCR and sRNA-seq. The expression levels of 7 identified miRNAs (miR-144, miR-124, miR-499, miR-125b, miR-430b, miR-430c and miR-152) were consistent with those determined by sRNA-seq. At DKA-exposure concentrations of 6.25 and 12.5 mg/L, 7 miRNAs were up-regulated, among which 5 miRNAs (miR-124, miR-499, miR-125b, miR-430c and miR-152) were concentration-dependent and 4 miRNAs (miR-137, miR-203b, miR-155 and miR-737) were inconsistent between sRNA-seq and qRT-PCR. For qRT-PCR analysis, miR-137, miR-203b, miR-155 and miR-737 were all up-regulated in the 6.25 mg/L treatment, but miR-155 was down-regulated in the 12.5 mg/L treatment. For sRNA-seq analysis, up-regulation of miR-137 and miR-737, as well as down-regulation of miR-203b and miR-155, was observed in the 6.25 mg/L treatment. In contrast, up-regulation of miR-137, miR-203b and miR-737, as well as down-regulation of miR-155, was observed in the 12.5 mg/L treatment (Fig. 2). These results demonstrate that different DKA concentrations lead to contrasting differential expressions of miRNAs in zebrafish.

3.5. Potential target gene prediction for significantly differential expression and high-abundance miRNAs, and cluster and pathway analyses

Cluster analyses of the 11 miRNAs provided important information for understanding differential expression between treatment and control groups (Table 1). Some miRNAs were up-regulated, while others were down-regulated (Fig. 3A). To better understand the biological functions of the 11 significantly differential expression and high-abundance miRNAs, we predicted their potential target genes and pathways using DIANA miRPath (v.2.0) (Fig. 3B). Through miRNA-targeted pathway union analysis, we found 8 major significant KEGG pathways (Fisher Exact Probability Test, $p < 0.05$) related to genes targeted by the 11 miRNAs. Several of the pathways were involved in cancer, hepatitis B, cell cycle, Salmonella infection, etc.

We also performed hierarchical clustering of differentially expressed miRNAs and their target pathways to further classify and predict the functions of differentially expressed miRNAs. The miRNAs with the same regulation pattern or similar functions were clustered together (Fig. 3B). According to the principles of lowest energy and highest score value in targetscan database analysis (http://www.targetscan.org/fish_62/), we predicted the 3′-UTR binding information for the most effective target genes of the 11 miRNAs. Table S4 summarizes the homology comparisons of the 11 miRNAs from zebrafish, human and mouse. By homology comparisons, the selected miRNAs were highly conserved in evolution, suggesting that they might have similar functions and metabolic

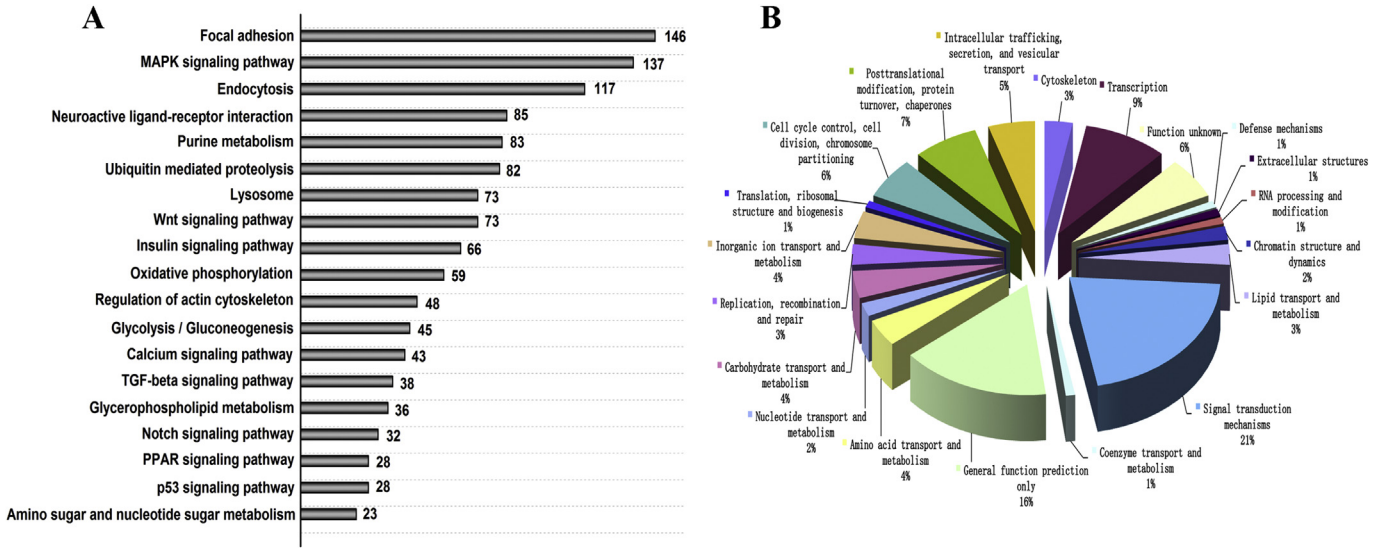

Fig. 1. (A) The number of miRNA predicted target genes mapped by pathway; (B) COG analysis of differentially expressed genes.

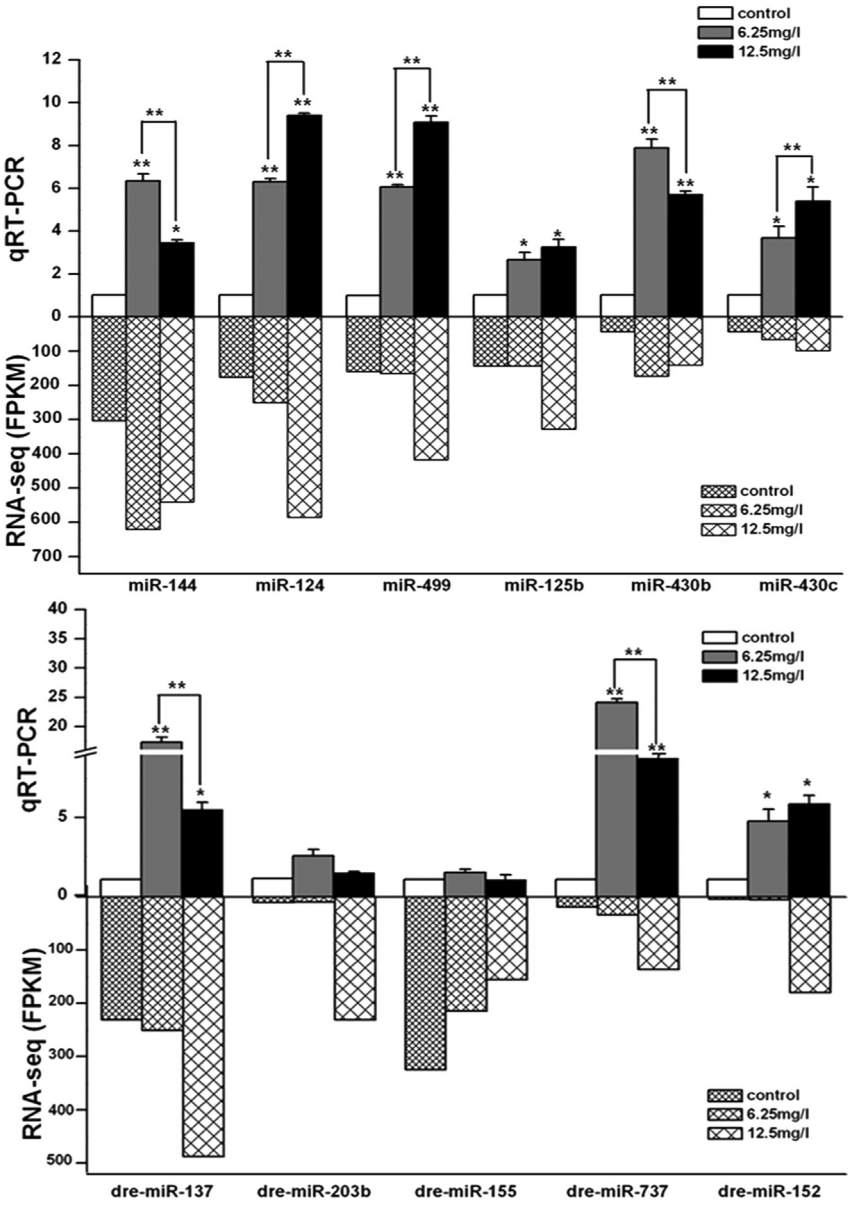

Fig. 2. The differential expression of the 11 significantly differential expression and high-abundance miRNAs for the control and DKA-exposed treatments by qRT-PCR. **Note**: (1) $^{*}p < 0.05$; (2) $^{**}p < 0.01$; (3) Significant level indicates comparisons between DKA-exposed treatment and control. (4) The statistical analyses in this figure were performed by post-hoc Tukey's tests.

pathways in zebrafish, as in human and mouse.

Fig. S5 shows a potential network between the 11 miRNAs and part of their target genes, which were differentially expressed and the most effective binding among all target genes. The diagram of the miRNA gene regulatory network quantitatively separates the core regulatory functions of miRNAs and their target genes. The high degree of connectivity between the miRNA-gene pairs suggests that these miRNAs play critical roles during zebrafish development.

3.6. Expression distribution and changes of miRNAs in F1-zebrafish by W-ISH

We performed W-ISH to verify the expression location, distribution and changing trend of miR-124 and miR-499 in F1-zebrafish. Results showed that the two miRNAs were mainly distributed in the liver, brain, gills, reproductive tract and cloaca. The expression of miR-124 and miR-499 in W-ISH was in general agreement with those from qRT-PCR and miRNA-seq. In control group, both of the miRNAs showed low expression in the brain, gilland lateral line neuromast in 7-dpf F1-zebrafish. In comparison, DKA-exposure led to the relatively high expression of miR-124 and miR-499 (Fig. 4A–B). Similarly, we performed ISH to confirm the tissue expression of miR-125b and miR-430c in F0-zebrafish ovary. The expression changes of miR-125b and miR-430c in ISH were generally consistent with those in qRT-PCR and miRNA-seq (Fig. 4C–D). In the mature follicle, the expression levels of miR-125b and mir-430c increased with increasing DKA-exposure concentrations, especially for the 12.5 mg/L treatment. The 12.5 mg/L treatment led to significantly increased fluorescence intensities compared with the control in F0-zebrafish ovary, while the trend diminished in the 6.25 mg/L treatment (Fig. 4E). In the vitellogenic

Table 1
Detailed information for the 11 miRNAs.

dre-miRNA	Ref miRNA	Group	miR-Locus	Control (A)	6.25 mg/L (B)	12.5 mg/L (C)	$\log_2$(fold change)		*p*-value (chi_square_2 × 2)		Mature sequence
							B/A	C/A	B/A	C/A	
dre-miR-152	hsa-miR-152	gp1		4.81	5.11	179.42	0.09	5.22	0.88219	1.6563E-47	UCAGUGCAUGACAGAACUUUGG
dre-miR-144	hsa-miR-144	gp1		303.56	619.61	540.25	1.03	0.83	9.4299E-28	9.4299E-28	UACAGUAUAGAUGAUGUACU
dre-miR-430b	hsa-miR-4735	gp1	chr4(+):28005855-28005926	43.06	173.00	141.44	2.00	1.72	1.1156E-18	1.1156E-18	CAACUCUAACUUUAGCAUCUUUC
dre-miR-430c	hsa-miR-520d	gp1		42.47	66.41	98.55	0.64	1.21	0.013467	1.1054E-09	UAAGUGCUUCUCUUUGGGGUAG
dre-miR-137	hsa-miR-137	gp1	chr2(−):18658740-18658830	230.62	251.32	488.14	0.12	1.08	0.18864	6.4147E-37	UUAUUGCUUAAGAAUACGCGUA
dre-miR-125b	hsa-miR-125b	gp1	chr5(+):31637249-31637340	143.92	142.01	327.20	−0.02	1.18	0.86251	6.7563E-28	UCCCUGAGACCCUAACUUGUGA
dre-miR-203b	hsa-miR-203b	gp1		10.62	9.20	231.13	−0.21	4.44	0.80705	8.1176E-58	GUGAAAUGUUCAGGACCACUUG
dre-miR-155	hsa-miR-155	gp1	chr1(+):451103-451202	324.40	214.54	155.98	−0.60	−1.06	0.000014238	1.4484E-07	UUAAUGCUAAUCGUGAUAGGGG
dre-miR-499	dre-miR-499a	gp1	chr11(−):26138745-26138841	159.84	164.48	416.18	0.04	1.38	0.57378	2.7537E-41	UUAAGACUUGCAGUGAUGUUUA
dre-miR-124	hsa-miR-124	gp1	chr20(−):38930194-39930283	276.04	387.71	646.95	0.49	1.23	1.8306E-06	1.1552E-55	UAAGGCACGCGGUGAAUGCCAA
dre-miR-737	NA	gp1		18.87	33.71	136.48	0.84	2.85	3.0057E-02	1.1182E-27	GUUUUUUUAGGUUUUGAUUUU

Note: The *p*-value was calculated by the following formula: $P(x,y) = \left(\frac{N2}{N1}\right)^{y} \frac{(x+y)!}{x!y!\left(1+\frac{N2}{N1}\right)^{(x+y+1)}}$ with a Python script.

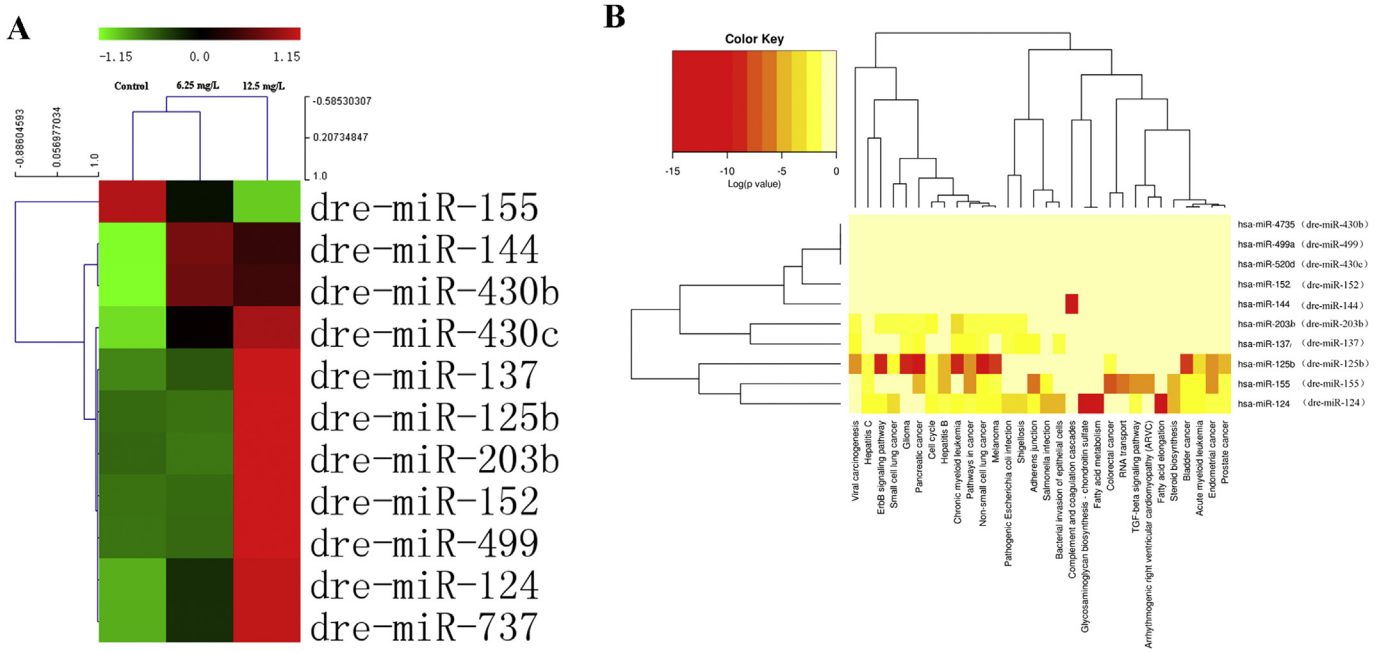

Fig. 3. (A) Cluster analyses of 11 significantly differential expression and high-abundance miRNAs; (B) Heat map and cluster patterns of the significantly differential expression and high-abundance miRNAs and target gene-related pathways. **Note**: (1) Colors distinguish differences in the expression of miRNAs. Red indicates high expression, while Green represents low expression; (2) In heat map of miRNAs versus pathways, miRNAs are clustered together by exhibiting similar pathway targeting patterns, and pathways are clustered together by related miRNAs; (3) As zebrafish genes were not included in the current version of DIANA miRPath, prediction was performed using human miRNAs. (For interpretation of the references to colour in this figure legend, the reader is referred to the web version of this article.)

follicle, the expression of miR-125b was very low and showed no significant difference ($p < 0.05$) compared to the control group. In contrast, miR-430c expression increased significantly ($p < 0.05$) with increasing DKA-exposure concentrations in the vitellogenic follicle (Fig. 4E). Abnormal expression of miR-125b and miR-430c could induce cancer in female zebrafish.

3.7. Histopathological analysis of F0-zebrafish ovary

Histopathological observations of F0-zebrafish ovary paraffin sections were conducted by microscope after 90 days of DKA exposure (0, 6.25 and 12.5 mg/L). DKA exposure induced severe histopathological changes and damage in zebrafish ovary tissue. Under 40× magnification, the ovary structure in the control group

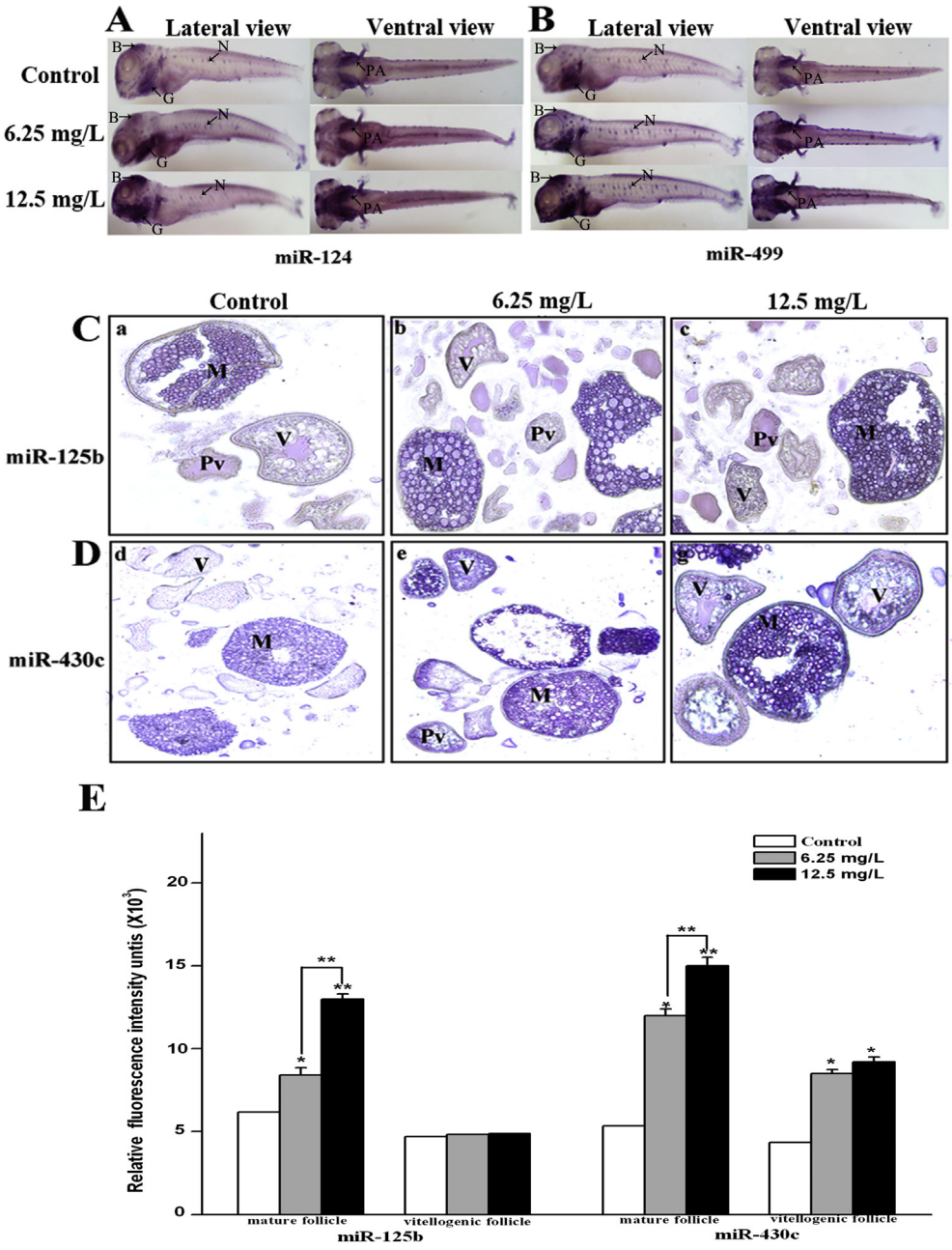

Fig. 4. (A) Whole-mount *in situ* hybridization of miR-124 expression in 7-dpf F1-zebrafish; (B) Whole-mount *in situ* hybridization of miR-499 expression in 7-dpf F1-zebrafish; (C) *in situ* hybridization of miR-125b expression in F0-zebrafish ovary; (D) *in situ* hybridization of miR-430c expression in F0-zebrafish ovary; (E) The relative fluorescence intensity units of miR-125b and miR-430c. **Note**: (1) B, brain; (2) G, gill; (3) PA, pharyngeal arches; (4) N, neuromast; (5) M, mature follicle; (6) V, vitellogenic follicle; (7) PV, previtellogenic follicle; (8) The statistical analyses in this figure were performed by post-hoc Tukey's tests.

was complete and clear, and the shape of oocytes was regular (Fig. 5A-a). In the 6.25 mg/L treatment, ovarian structure was relatively complete, cell gap became large and cell distribution was scattered (Fig. 5B-b). In sharp contrast in the 12.5 mg/L treatment, the ovary structure changed significantly, reflected by an increased number of early developmental oocytes, irregular cell distribution, different cellular morphology, decreased yolk granules, cytoplasmic shrinkage and cell lysis in mature oocytes (Fig. 5A–C). Transmission electron microscopy (TEM) was used to analyze histopathological alterations of F0-zebrafish ovary. Zebrafish ovary suffered serious damage in both 6.25 and 12.5 mg/L treatments. In normal yolk, the electron density was uniform and the external corona radiata (ECR) was thin with a high electron density. The internal corona radiata (ICR) was wide and close to the egg membrane of the oocyte (Fig. 5B-a and B-d). In contrast, after DKA exposure, the yolk shrank and displayed oedematous (Fig. 5B-b and B-c), the ICR became narrow concomitant with dissolution phenomenon, and the ECR disappeared (Fig. 5B-e and B-f). The degree of damage to the ovary increased with increasing DKA-exposure concentrations. These histopathological phenomena demonstrate that chronic DKA exposure can seriously affect the reproduction of female zebrafish, including infertility.

4. Discussion

The previous studies on the toxicity of antibiotics were mainly

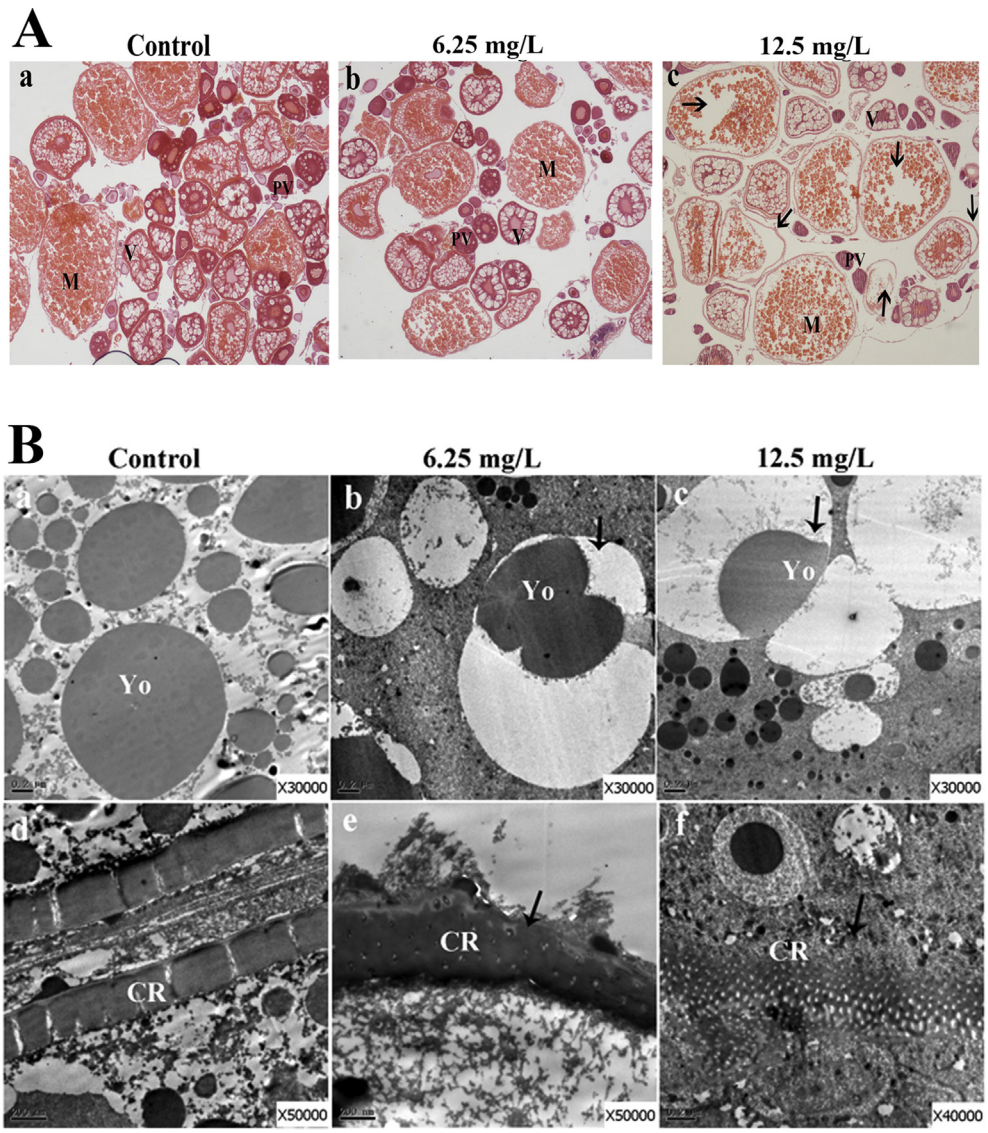

Fig. 5. Haematoxylin and eosin (HE) dyeing (A) and TEM images (B) of zebrafish ovary tissues. **Note**: (1) a, b and c represent the ovary structure in control, 6.25 mg/L treatment and 12.5 mg/L treatments, respectively; (2) M, mature follicle; (3) V, vitellogenic follicle; (4) PV, previtellogenic follicle; (5) Yo, yolk; (6) Cr, corona radiata; (7) a, normal yolk of oocyte; (8) b-c, shrinking and oedematous yolk in 6.25 and 12.5 mg/L treatments; (9) d, normal corona radiata; (10) e, narrow internal corona radiata concomitant with dissolution phenomenon in 6.25 mg/L treatment; (11) f, disappearance of external corona radiata in 12.5 mg/L treatment.

focused on the toxicological analysis and the related mechanism for single DKA species (Yin et al., 2006). Because many kinds of DKAs co-exist in real-world aquatic environment, their interaction may have additive, synergistic or antagonistic effects. *In vivo* experiments, the transformation and different distribution of DKAs in the organism lead to the research more complicated. Therefore, it is necessary to study the joint effects of DKAs to accurately evaluate their ecological risk. The present study selected three FQs and three TCs as representative DKA species because they are frequently detected in aquatic environments (Zhang et al., 2016). Our group previously investigated the effects of FQs, TCs and their mixtures on zebrafish growth, development and behavior, and found that FQs and TCs had the synergistic effects on mortality, malformation and hatching rates. The acute DKA-exposure of FQs caused no obvious malformation, but TCs resulted in severe abnormality such as hatching delay, uninflated swim bladder, yolk sac edema, pericardial edema and crooked body (Zhang et al., 2016; Wang et al., 2014). The molecular mechanism on the above malformation phenomenon is required to be further investigated.

Currently, sRNA high throughput sequencing is widely applied for studying biological responses in various animals, plants and bacteria. These studies provide valuable information on miRNAs regulatory networks in response to environmental stressors. In current study, the significantly differential expression and high-abundance miRNAs were screened and a small RNA library was constructed from 7-dpf F1-zebrafish by using miRNA high throughput sequencing after DKA exposure to F0 zebrafish. Based on miRNAs-seq quality control, we screened 193 significant differential miRNAs with $|\text{fold change}| \geq 1$ and p-value ≤ 0.05. Subsequently, we selected high-abundance miRNAs to further conduct verification of their abnormal expression by means of qRT-PCR and W-ISH. These results preliminarily illustrated the toxic effect transfer relation across parent and their offspring. That was to say that F1-zebrafish abnormal development was closely concerned with damage to F0-zebrafish reproductive organs due to chronic DKA exposure. The test results of phenotypic characteristics

showed that although chronic DKA exposure did not result in an obvious malformation and lethal phenomena, abnormality changes in some molecular targets and tissue damage to reproductive organs occurred. As a result, these observations play a caution function for the sake of studying reproductive toxicity of trace-level environmental pollutants. Our previous researches demonstrated that DKA exposure at trace level caused behavioral abnormality of F1- and F0-zebrafish, the decreased fecundity and hatching rate and the increased larval mortality rate (Zhang et al., 2016). These data disclosed the reproductive toxicity of DKAs and the related molecular targets of DKAs at molecular level.

COG protein classification disclosed that one of the prominent functions for proteins regulated by the differentially expressed genes was signal transduction. In this investigation examining exposure to DKAs, annotation of target genes demonstrated that they played important roles in endocrine system disrup-Tion, immune systems and reproductive activity. The expression levels of 7 identified miRNAs were consistent with those by sRNA-seq, and 4 miRNAs (miR-499, miR-124, miR-430c and mir-125b) were screened to explore their effects on the reproductive system following exposure to DKAs. MicroRNA-124 is the most abundant miRNA in the central nervous system (CNS) and nerve cells, and it is 100 times higher in the CNS than in other body tissues (Hamzei et al., 2016). It is expressed strongly and abundantly in brain tissue and can effectively protect neuron apoptosis caused by cerebral apoplexy (Shao et al., 2015). MicroRNA-124 as a tumor suppressor can inhibit cell proliferation, migration and invasion in human lung adenocarcinoma by directly targeting SOX9, which is a promising candidate for miRbased therapy against lung adenocarcinoma tissues (Wang et al., 2016a,b). Dysregulation of miR-124 can result in initiation and progression of cancer. Sato et al. (2015) reported that serum miR-124 concentration can be used as a disease activity marker for severe drug eruptions, reflecting the severity of keratinocyte apoptosis and miR-124 up-regulation as a disease marker of toxic epidermal necrolysis. MicroRNA-124 is related to podocytic adhesive capacity damage and may be implicated in the pathogenesis of diabetic nephropathy (Li et al., 2013a,b). In this study, we found the expression of miR-124 was significantly up-regulated in F1-zebrafish under DKA exposure, which may be a disease marker.

MicroRNA-499 is abundantly expressed in the myocardium and is thus called cardiac miRNAs, which plays a central role in cardiogenesis, heart function and pathology (Chistiakov et al., 2016). It is increased in human and murine cardiac hypertrophy and cardiomyopathy, is sufficient to cause murine heart failure, and accelerates maladaptation to pressure overloading (Matkovich et al., 2012). Over-expression of miR-499 protects cardiomyocytes against lipopolysaccharide- induced apoptosis (Jia et al., 2016). MicroRNA-499mutation conditionally changes miR-499 target mRNA recognition, thereby altering the effects of miR-499 on cardiac transcriptome and proteome and modifies characteristics of the cardio-myopathy conferred by miR-499 over-expression (Dorn et al., 2012). Sox6 is believed to be one of the miR-499 targets, and also to play a key role in cardiac differentiation (Li et al., 2013a,b).

The over-expression of miR-430 in human bladder cancer 5637 cells significantly inhibited cell proliferation, migration and colony formation efficiency (Liu et al., 2013). The miR-430 precursors were classified as miR-430a, miR-430b, miR-430c and miR-430d (Mishima et al., 2006). Previous reports have shown that miR-430 target mRNAs are equally susceptible to repression in somatic cells and primordial germ cells (Giraldez et al., 2006). *Cyp19b* is a target gene of the miR-430 family. The transcription factor Foxl2 is characterized as an ovarian-specific upstream regulator of the *cyp19a* promoter that co-activates *cyp19a* expression and plays an important role in gonadal differentiation and development (Kedde et al., 2007).

As for miRNAs in female reproductive tissue, most work had focused on miRNA profiling rather than mechanism, and miR-125b was reported to be one of the most abundant miRNAs in the ovary among different species (Donadeu et al., 2012; Hossain et al., 2013). MicroRNA-125b has been demonstrated to be down-regulated in certain types of cancer, such as bladder cancer, thyroid anaplastic carcinomas, squamous cell carcinoma of the tongue, hepatocellular carcinoma, and ovarian and breast cancer (Wu et al., 2013). Overexpression of miR-125b represses the endogenous level of p53 protein and suppresses apoptosis in human neuroblastoma cells and human lung fibroblast cells. MiR-125b is an important negative regulator of *p53* and *p53*-induced apoptosis during development and stress response (Le et al., 2009).*Blc3* as an oncogene was observed to be down-regulated by miR-125b at the translational level in ovarian cancer cells (Guan et al., 2011). Previous research suggests that PPARγ could induce growth suppression of ovarian cancer cells by up-regulating miR-125b and inhibiting proto-oncogene BCL3 (Luo et al., 2015). Receptor tyrosine kinases ERBB2 and ERBB3 were shown to be targets of miR-125a/b, and overexpression of miR-125a/b in an ERBB2-positive breast cancer cell line impaired cell growth and mobility capability (Scott et al., 2007). Frequent overexpression or amplification of ERBB2 was reported in ca. 20% of serous ovarian cancers (Lassus et al., 2004). In this investigation, we found that DKA exposure resulted in overexpression of miR-125b in F0-zebrafish ovary, which could lead to occurrence of cancer. Therefore, we conclude that DKA exposure elicits a reproductive toxicity response.

5. Conclusions

In this study, small RNA high-throughput sequencing technology was used to characterize the miRNAs in F1-zebrafish after 90-day DKA exposure to F0-zebrafish at 6.25 and 12.5 mg/L. Among control and DKA-exposed groups, 193 mature miRNAs were found to be differentially expressed (p-value ≤ 0.05, $|\text{fold change}| \geq 1$), and they were classified as either conserved miRNAs or non-annotated sRNAs. When referenced to three databases, 2523 potential target genes were successfully predicted. The expression levels of 7 identified miRNAs (miR-144, miR-124, miR-499, miR-125b, miR-430b, miR-430c and miR-152) assessed by qRT-PCR were consistent with those determined by sRNA-seq. A diagram for the miRNA gene regulatory network was plotted, and the high-degree of connectivity between miRNA-gene pairs suggests that these miRNAs play critical roles during zebrafish development. The expression of miR-124 and miR-499 in whole-mount *in situ* hybridization was generally consistent with those in qRT-PCR and miRNA-seq. The expressions of miR-124 and miR-499 increased with increasing DKA-exposure concentrations. DKA exposure resulted in severe histopathological changes and damage to F0-zebrafish ovary. These observations demonstrated that chronic DKA exposure can seriously impact reproduction of F0-zebrafish and development of F1-zebrafish.

Acknowledgement

This work is jointly supported by the National Natural Science Foundation of China (31270548, and 21377100), the Natural Science Foundation of Zhejiang Province (LY15C030004 and LY15B070009), the Public Beneficial Project of Wenzhou City Sci & Technol Bureau (H20150005 and Y20150001), and Zhejiang Provincial Xinmiao Talent Project (2016R413084).

Appendix A. Supplementary data

Supplementary data related to this article can be found at http://

dx.doi.org/10.1016/j.chemosphere.2016.07.057.

References

Alavi, N., Babaei, A.A., Shirmardi, M., Naimabadi, A., Goudarzi, G., 2015. Assessment of oxytetracycline and tetracycline antibiotics in manure samples in different cities of Khuzestan province. Iran. Environ. Sci. Pollut. Res. Int. 22, 17948–17954.

Ambili, T.R., Saravanan, M., Ramesh, M., Abhijith, D.B., Poopal, R.K., 2012. Toxicological effects of the antibiotic oxytetracycline to an Indian major carp *Labeo rohita*. Arch. Environ. Contam. Toxicol. 64, 494–503.

Bhattacharya, M., Sharma, A.R., Sharma, G., Patra, B.C., Nam, J.S., Chakraborty, C., Lee, S.S., 2016. The crucial role and regulations of miRNAs in zebrafish development. Protoplasma 30, 1–15.

Brown, K.D., Kulis, J., Thomson, B., Chapman, T.H., Mawhinney, D.B., 2006. Occurrence of antibiotics in hospital, residential, and diary effluent, municipal wastewater, and the Rio Grande in New Mexico. Sci. Total Environ. 366, 772–783.

Chistiakov, D.A., Orekhov, A.N., Bobryshev, Y.V., 2016. Cardiac-specific miRNA in cardiogenesis, heart function, and cardiac pathology (with focus on myocardial infarction). J. Mol. Cell. Cardiol. 94, 107–121.

Donadeu, F.X., Schauer, S.N., Sontakke, S.D., 2012. Involvement of miRNAs in ovarian follicular and luteal development. J. Endocrinol. 215, 323–334.

Dorn, G.W., Matkovich, S.J., Eschenbacher, W.H., Zhang, Y., 2012. A human 3′ miR-499 mutation alters cardiac mRNA targeting and function. Circ. Res. 110, 958–967.

Farombi, E.O., Ugwuezunmba, M.C., Ezenwadu, T.T., Oyeyemi, M.O., Ekor, M., 2008. Tetracycline-induced reproductive toxicity in male rats: effects of vitamin C and N-acetylcysteine. Exp. Toxicol. Pathol. 60, 77–85.

Fu, H.J., Zhu, J., Yang, M., Zhang, Y.Z., Tie, Y., Jiang, H., Sun, X.Z., Zheng, F.X., 2006. A novel method to monitor the expression of microRNAs. Mol. Biotechnol. 32, 197–204.

Giraldez, A.J., Mishima, Y., Rihel, J., Grocock, R.J., Dongen, S.V., Inoue, K., Enright, A.J., Schier, A.F., 2006. Zebrafish miR-430 promotes deadenylation and clearance of maternal mRNAs. Science 312, 75–79.

Golet, E.M., Alder, A.C., Hartmann, A., Ternes, T.A., Giger, W., 2001. Trace determination of fluoroquinolone antibacterial agents in urban waste water by solid-phase extraction and liquid chromatography with fluoroquinolone detection. Anal. Chem. 73, 3632–3638.

Guan, Y., Yao, H., Zheng, Z., Qiu, G., Sun, K., 2011. miR-125b targets *Bcl3* and suppresses ovarian cancer proliferation. Int. J. Cancer 128, 2274–2283.

Hagenbuch, I.M., Pinckney, J.L., 2012. Toxic effect of the combined antibiotics ciprofloxacin, lincomycin, and tylosin on two species of marine diatoms. Water. Res. 46, 5028–5036.

Hamzei, T.S., Kho, W., Riou, A., Wiedermann, D., Hoehn, M., 2016. miRNA-124 induces neuroprotection and functional improvement after focal cerebral ischemia. Biomaterials 91, 151–165.

Hossain, M.M., Cao, M., Wang, Q., Kim, J.Y., Schellander, K., Tesfaye, D., Tsang, B.K., 2013. Altered expression of miRNAs in a dihydrotestosterone-induced rat PCOS model. J. Ovarian Res. 6, 1–11.

Huang, C., Dong, Q., Walter, R.B., Tiersch, T.R., 2004. Sperm cryopreservation of green swordtail *Xiphophorus helleri*, a fish with internal fertilization. Cryobiology 48, 295–308.

Huang, D.W., Sherman, B.T., Lempicki, R.A., 2009. Bioinformatics enrichment tools: paths toward the comprehensive functional analysis of large gene lists. Nucleic Acids Res. 37, 1–13.

Jia, Z., Wang, J., Shi, Q., Liu, S., Wang, W., Tian, Y., Lu, Q., Chen, P., Ma, K., Zhou, C., 2016. *SOX6* and *PDCD4* enhance cardiomyocyte apoptosis through LPS-induced miR-499 inhibition. Apoptosis 21, 174–183.

Kedde, M., Strasser, M.J., Boldajipour, B., Oude Vrielink, J.A., Slanchev, K., le Sage, C., Nagel, R., Voorhoeve, P.M., van Duijse, J., Ørom, U.A., Lund, A.H., Perrakis, A., Raz, E., Agami, R., 2007. RNA-binding protein Dnd1 inhibits microRNA access to target mRNA. Cell 131, 1273–1286.

Khor, E.S., Noor, S.M., Wong, P.F., 2016. Expression of zTOR-associated microRNAs in zebrafish embryo treated with rapamycin. Life Sci. 150, 67–75.

Krol, J., Loedige, I., Filipowicz, W., 2010. The widespread regulation of microRNA biogenesis, function and decay. Nat. Rev. Genet. 11, 597–610.

Le, M.T., Teh, C., Shyh-Chang, N., Xie, H., Zhou, B., Korzh, V., Lodish, H.F., Lim, B., 2009. microRNA-125b is a novel negative regulator of p53. Genes Dev. 23, 862–876.

Li, D., Lu, Z., Jia, J., Zheng, Z., Lin, S., 2013a. miR-124 is related to podocytic adhesive capacity damage in STZ-induced uninephrectomized diabetic rats. Kidney Blood Press. Res. 37, 422–431.

Lindberg, R., Jarnheimer, P.A., Olsen, B., Johansson, M., Tysklind, M., 2004. Determination of antibiotic substances in hospital sewage water using solid phase extraction and liquid chromatography mass spectrometry and group analogue internal standards. Chemosphere 57, 1479–1488.

Liu, L., Zhao, X., Zhu, X., Zhong, Z., Xu, R., Wang, Z., Cao, J., Hou, Y., 2013. Decreased expression of miR-430 promotes the development of bladder cancer via the upregulation of *CXCR7*. Mol. Med. Rep. 8, 140–146.

Li, X., Wang, J., Jia, Z., Cui, Q., Zhang, C., Wang, W., Chen, P., Ma, K., Zhou, C., 2013b. miR-499 regulates cell proliferation and apoptosis during late-stage cardiac differentiation via *Sox6* and cyclin D1. PLoS One 8, e74504.

Luo, S., Wang, J., Ma, Y., Yao, Z., Pan, H., 2015. PPARγ inhibits ovarian cancer cells proliferation through upregulation of miR-125b. Biochem. Biophys. Res. Commun. 462, 85–90.

Lassus, H., Leminen, A., Vayrynen, A., Cheng, G., Gustafsson, J.A., Isola, J., Butzow, R., 2004. ERBB2 amplification is superior to protein expression status in predicting patient outcome in serous ovarian carcinoma. Gynecol. Oncol. 92, 31–39.

Matkovich, S.J., Hu, Y., Eschenbacher, W.H., Dorn, L.E., Dorn, G.W., 2012. Direct and indirect involvement of microRNA-499 in clinical and experimental cardiomyopathy. Circ. Res. 111, 521–531.

Melvin, S.D., Cameron, M.C., Lanctot, C.M., 2014. Individual and mixture toxicity of pharmaceuticals naproxen, carbamazepine, and sulfamethoxazole to Australian striped marsh frog tadpoles (*Limnodynastes peronii*). J. Toxicol. Environ. Health A 77, 337–345.

Mishima, Y., Giraldez, A.J., Takeda, Y., Fujiwara, T., Sakamoto, H., Schier, A.F., Inoue, K., 2006. Differential regulation of germline mRNAs in soma and germ cells by zebrafish miR-430. Curr. Biol. 16, 2135–2142.

Mohan, J., Sastry, K.V., Tyagi, J.S., Singh, D.K., 2004. Isolation of *E. colifrom* foam and effect of fluoroquinolones on *E. coli* and foam production in male Japanese quail. Theriogenology 62, 1383–1390.

Sato, S., Ichihara, A., Jinnin, M., Izuno, Y., Fukushima, S., Ihn, H., 2015. Serum miR-124 up-regulation as a disease marker of toxic epidermal necrolysis. Eur. J. Dermatol. 25, 457–462.

Scott, G.K., Goga, A., Bhaumik, D., Berger, C.E., Sullivan, C.S., Benz, C.C., 2007. Coordinate suppression of ERBB2 and ERBB3 by enforced expression of micro-RNA miR-125a or miR-125b. J. Biol. Chem. 282, 1479–1486.

Sendzik, J., Shakibaei, M., Schäfer-Korting, M., Lode, H., Stahlmann, R., 2010. Synergistic effects of dexamethasone and quinolones on human-derived tendon cells. Int. J. Antimicrob. Agents 35, 366–374.

Shao, Q., Jiang, W., Jin, Y., 2015. miR-124 effect in neurons apoptosis in newborn rat with thyroid hypofunction. Int. J. Clin. Exp. Pathol. 8, 14465–14471.

Sipes, N.S., Padilla, S., Knudsen, T.B., 2011. Zebrafish: as an integrative model for twenty-first century toxicity testing. Birth Defects Res. Part C 93, 256–267.

Thisse, C., Thisse, B., 2008. High-resolution *in situ* hybridization to whole-mount zebrafish embryos. Nat. Protoc. 3, 59–69.

Vlachos, I.S., Kostoulas, N., Vergoulis, T., Georgakilas, G., Reczko, M., Maragkakis, M., Paraskevopoulou, M.D., Prionidis, K., Dalamagas, T., Hatzigeorgiou, A.G., 2012. DIANA miRPath v.2.0: investigating the combinatorial effect of microRNAs in pathways. Nucleic Acids Res. 40, 498–504.

Wang, H.L., Che, B.G., Duan, A.L., Mao, J.W., Dahlgren, R.A., Zhang, M.H., Zhang, H.Q., Zeng, A.B., Wang, X.D., 2014. Toxicity evaluation of β-diketone antibiotics on the development of embryo larval zebrafish (*Danio rerio*). Environ. Toxicol. 29, 1134–1146.

Wang, X., Liu, Y., Liu, X., Yang, J., Teng, G., Zhang, L., Zhou, C., 2016a. miR-124 inhibits cell proliferation, migration and invasion by directly targeting *SOX9* in lung adenocarcinoma. Oncol. Rep. 35, 3115–3121.

Wang, X., Zheng, Y., Zhang, Y., Li, J., Zhang, H., Wang, H., 2016b. Effects of β-diketone antibiotic mixtures on behavior of zebrafish (*Danio rerio*). Chemosphere 144, 2195–2205.

Wu, D., Ding, J., Wang, L., Pan, H., Zhou, Z., Zhou, J., Qu, P., 2013. microRNA-125b inhibits cell migration and invasion by targeting matrix metallopeptidase 13 in bladder cancer. Oncol. Lett. 5, 829–834.

Yao, G., Yin, M., Lian, J., Tian, H., Liu, L., Li, X., Sun, F., 2010. microRNA-224 is involved in transforming growth factor-beta-mediated mouse granulosa cell proliferation and granulosa cell function by targeting *Smad4*. Mol. Endocrinol. 24, 540–551.

Yin, H.Q., Kim, M., Kim, J.H., Kong, G., Lee, M.O., Kang, K.S., Yoon, B.I., Kim, H.L., Lee, B.H., 2006. Hepatic gene expression profiling and lipid homeostasis in mice exposed to steatogenic drug, tetracycline. Toxicol. Sci. 94, 206–216.

Yoon, Y., Ryu, J., Oh, J., Choi, B.G., Snyder, S.A., 2010. Occurrence of endocrine disrupting compounds, pharmaceuticals, and personal care products in the Han River (Seoul, South Korea). Sci. Total Environ. 408, 636–643.

Zhang, Y.N., Wang, X., Yin, X., Shi, M., Dahlgren, R.A., Wang, H., 2016. Toxicity assessment of combined fluoroquinolone and tetracycline exposure in zebrafish (*Danio rerio*). Environ. Toxicol. 31, 736–750.

Zhao, X., Wang, X., Li, F., Dahlgren, R.A., Wang, H., 2015. Identification of microRNA-size sRNAs related to Salt Tolerance in *Spirulina platensis*. Plant Mol. Biol. Rep. 2015, 1–17.